Pergamon

0045-7949(94)00399-8

*Computers & Structures* Vol. 54, No. 6, pp. 1091–1097, 1995

0045-7949/95 $9.50 + 0.00

# A CO-ROTATIONAL FORMULATION FOR NONLINEAR DYNAMIC ANALYSIS OF CURVED EULER BEAM

**Kuo Mo Hsiao** and **Rong Tser Yang**

Department of Mechanical Engineering, National Chiao Tung University, 1001 Ta Hsueh Road, Hsinchu, Taiwan, Republic of China

(*Received* 31 *October* 1993)

**Abstract**—A co-rotational finite element formulation for the dynamic analysis of a planar curved Euler beam is presented. The Euler–Bernoulli hypothesis and the initial curvature are properly considered for the kinematics of a curved beam. Both the deformational nodal forces and the inertial nodal forces of the beam element are systematically derived by consistent linearization of the fully geometrically nonlinear beam theory in element coordinates which are constructed at the current configuration of the corresponding beam element. An incremental-iterative method based on the Newmark direct integration method and the Newton–Raphson method is employed here for the solution of the nonlinear dynamic equilibrium equations. Numerical examples are presented to demonstrate the effectiveness of the proposed element and to investigate the effect of the initial curvature on the dynamic response of the curved beam structures.

## 1. INTRODUCTION

The nonlinear dynamic behavior of beam structures, e.g. framed structures, flexible mechanisms, and robot arms, has been the subject of considerable research. Currently, the most popular approach for this analysis is to develop finite element models. Several studies have been made on investigating the dynamic response of flexible beams subject to large rigid body motion and small elastic deformations [1–14]. However, almost all of these studies are limited to the analysis of a straight beam or a slender curved beam. The circumferential strain varies linearly with distance from the centroid of the cross section for a straight beam, but does not vary linearly for a curved beam. In [3, 4, 10, 13], the distribution of the circumferential strain in a curved beam was calculated by regarding the beam as straight. This approximation is accurate enough for slender curved beams in which the product of the initial curvature and the depth of the cross section is much smaller than unity. When this product is not much smaller than unity, the strains in a curved beam differ significantly from the strains in a straight beam of the same cross section [15]. Hence, as this product increases, the accurate expression for the kinematics of a curved beam should be used to obtain a reliable dynamic response.

The objective of this study is to present a consistent co-rotational formulation for the dynamic analysis of a planar curved Euler beam with large rigid body motion and small elastic deformations. In order to capture all inertia effects and coupling between extensional and flexural deformations for a curved beam element, the inertia nodal forces and deformational nodal forces are systematically derived by consistent linearization [6, 14] of the fully geometrically nonlinear beam theory using the d'Alembert principle and the virtual work principle. Here, the Euler–Bernoulli hypothesis [14, 16] and the initial curvature are properly considered to obtain a correct expression for the kinematics of a curved beam. Following Hsiao and Jang [9, 12] the nodal coordinates, incremental displacements and rotations, velocities, accelerations, and the equations of motion of the system are defined in terms of a fixed global coordinate system, while the total strains in the beam element are measured in element coordinates which are constructed at the current configuration of the beam element. The element equations are constructed first in the element coordinate system and then transformed to the global coordinate system using standard procedure. The dominant factors in the geometrical nonlinearities of beam structures are attributable to finite rotations, the strains remaining small. For a beam structure discretized by finite elements, this implies that the motion of the individual elements to a large extent will consist of rigid body motion. If the rigid body motion part is eliminated from the total displacements and the element size is properly chosen, the deformational part (initial deformation included) of the motion is always small relative to the local element axes; thus in conjuction with the co-rotational formulation, the higher order terms of nodal parameters in the element deformational nodal forces and inertia nodal forces may be neglected.

An incremental-iterative method based on the Newmark direct integration method and the Newton–Raphson method is employed here for the solution of the nonlinear dynamic equilibrium equations. Numerical examples are presented to demonstrate the effectiveness and versatility of the

proposed beam element for the dynamic analysis of the beam structures and to investigate the effect of the initial curvature on the dynamic response of the curved beam structures.

## 2. NONLINEAR FORMULATION

### 2.1. *Basic assumptions*

The following assumptions are made in derivation of the nonlinear behavior.

(1) The Euler–Bernoulli hypothesis is valid.
(2) The unit extension of the centroid axis of the beam element is uniform.
(3) The deflections of the beam element measured in the element coordinates are small.
(4) The strain of the beam element is small.

The third assumption can always be satisfied if the element size is properly chosen. Due to the assumption of small strain, the engineering strain and stress are used for the measure of the strain and stress. For convenience, the engineering strain is obtained from the corresponding Green strain in this study.

### 2.2. *Coordinate systems*

In order to describe the system, following [9, 12], we define two sets of coordinate systems (see Fig. 1) as follows.

(1) A fixed global set of coordinates, $X_1$, $X_2$; the nodal coordinates, incremental displacements and rotations, velocities, accelerations, and the equations of motion of the system are defined in this coordinate system.
(2) Element coordinates, $x_1$, $x_2$; a set of element coordinates associated with each element, which is constructed at the current configuration of the beam element. The element equations are constructed first in the element coordinate system and then transformed to the global coordinate system using standard procedure.

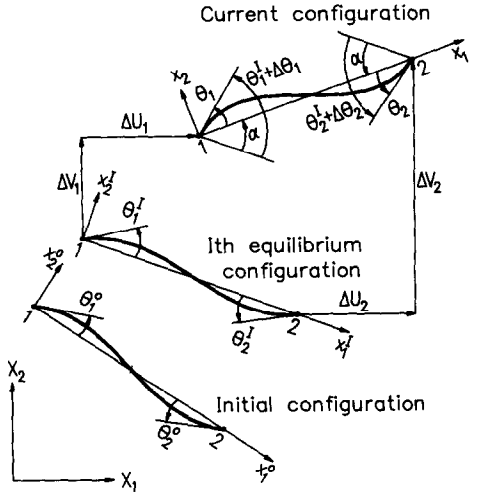


Fig. 1. Coordinate systems.

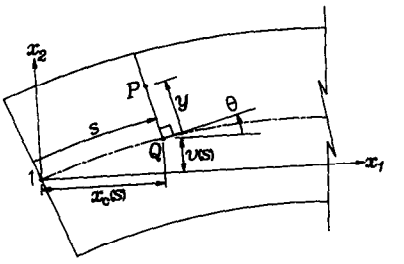


Fig. 2. Kinematics of the deformed beam.

### 2.3. *Kinematics of beam elements*

The geometry of the beam element is described in the current element coordinate system. In this study, the symbol { } denotes column matrix, and the symbol $\bar{(\ )}$ denotes the variable ( ) in the undeformed state. Let $P$ (Fig. 2) be an arbitrary point in the beam element, and $Q$ be the corresponding point of $P$ on the centroid axis. The position vector of point $P$ in the undeformed and deformed configurations can be expressed as

$$\bar{\mathbf{r}} = \{\bar{x}_p, \bar{y}_p\} = \{\bar{x}_c(\bar{s}) - y \sin\bar{\theta}, \bar{v}(\bar{s}) + y\cos\bar{\theta}\} \quad (1)$$

and

$$\mathbf{r} = \{x_p, y_p\} = \{x_c(s) - y\sin\theta, v(s) + y\cos\theta\} \quad (2)$$

where $x_c(s)$ and $v(s)$ are the $x_1$ and $x_2$ coordinates of point $Q$, respectively, $s$ is the arc length of the deformed centroid axis measured from node 1 to point $Q$, $y$ is the distance between points $P$ and $Q$, and $\theta$ is the angle measured from the $x_1$ axis to the tangent of the centroid axis. The relationship among $x_c(s)$ and $v(s)$ and $s$ may be given as

$$x_c(s) = u_1 + \frac{S}{2}\int_{-1}^{\xi} \cos\theta \, d\xi, \quad (3)$$

where

$$\cos\theta = (1 - v'^2)^{1/2} \quad (4)$$

$$v' = \frac{dv(s)}{ds} = \sin\theta \quad (5)$$

and

$$\xi = -1 + \frac{2s}{S}, \quad (6)$$

in which $u_1$ is the displacement of node 1 in the $x_1$ direction. $S$ is the current arc length of the centroid axis of the beam element. Note that due to the definition of the element coordinate system, the value of $u_1$ is equal to zero. However, the variations of $u_1$ are not zero. Making use of eqn (3), we obtain

$$S = \frac{2l}{\beta}, \quad (7)$$

where

$$\beta = \int_{-1}^{1} \cos\theta \, d\xi \tag{8}$$

and

$$l = x_c(S) - x_c(0) = L - u_1 + u_2, \tag{9}$$

in which $l$ is the current chord length of the beam axis, $L$ is the chord length of the undeformed beam axis, and $u_2$ is the displacement of node 2 in the $x_1$ direction.

If $\bar{s}$ and $y$ in eqn (1) are regarded as the independent variables, the Green strains $\epsilon_{ij}$ $(i = 1, 2, j = 1, 2)$ are given by [17]

$$\epsilon_{ij} = \tfrac{1}{2}(\mathbf{G}_i^{\mathrm{T}}\mathbf{G}_j - \mathbf{g}_i^{\mathrm{T}}\mathbf{g}_j), \tag{10}$$

where

$$\mathbf{G}_1 = \frac{\partial \mathbf{r}}{\partial \bar{s}} = \frac{\partial \mathbf{r}}{\partial \bar{s}}\frac{\partial s}{\partial \bar{s}} = (1-\epsilon_0)(1-\kappa y)\{\cos\theta, \sin\theta\}$$

$$\mathbf{G}_2 = \frac{\partial \mathbf{r}}{\partial y} = \{-\sin\theta, \cos\theta\}$$

$$\mathbf{g}_1 = \frac{\partial \bar{\mathbf{r}}}{\partial \bar{s}} = (1-\bar{\kappa}y)\{\cos\bar{\theta}, \sin\bar{\theta}\}$$

$$\mathbf{g}_2 = \frac{\partial \bar{\mathbf{r}}}{\partial y} = \{-\sin\bar{\theta}, \cos\bar{\theta}\} \tag{11}$$

$$\epsilon_0 = \frac{\partial s}{\partial \bar{s}} - 1 \tag{12}$$

and

$$\kappa = \frac{\delta\theta}{\partial s} = cv'', \tag{13}$$

in which

$$c = \frac{1}{\cos\theta} \tag{14}$$

$$v'' = \frac{d^2v}{ds^2}. \tag{15}$$

Note that $\kappa$ in eqn (13) is an exact expression for the physical curvature of the deformed beam centroid axis. An equivalent expression for $\kappa$ is given by Hodges [16]. Making use of the assumption of uniform unit extension, we may rewrite the unit extension $\epsilon_0$ in eqn (12) as

$$\epsilon_0 = \frac{S}{\bar{S}} - 1. \tag{16}$$

Due to the use of the Euler–Bernoulli hypothesis, as expected, $\epsilon_{11}$ is the only nonzero component of $\epsilon_{ij}$. Substituting eqn (11) into eqn (10) we may obtain

$$\epsilon_{11} = \tfrac{1}{2}[(1+\epsilon_0)^2(1-\kappa y)^2 - (1-\bar{\kappa}y)^2]. \tag{17}$$

The engineering strain corresponding to $\epsilon_{11}$ is given by [17]

$$\epsilon = \left(1 + \frac{2\epsilon_{11}}{\mathbf{g}_1^{\mathrm{t}}\mathbf{g}_1}\right)^{1/2} - 1 = \frac{(1+\epsilon_0)(1-\kappa y)}{(1-\bar{\kappa}y)} - 1. \tag{18}$$

Note that $\epsilon$ in eqn (18) is an exact expression of engineering strain for the curved Euler beam. Here, the lateral deflection of the centroid axis, $v(s)$, is assumed to be the cubic Hermitian polynomials of $s$ and is given by

$$v(s) = \{N_1, N_2, N_3, N_4\}^T\{v_1, v_1', v_2, v_2'\} = \mathbf{N}_{\mathbf{b}}^{\mathrm{T}}\mathbf{u}_{\mathbf{b}}, \tag{19}$$

where $v_j$ and $v_j'$ $(j = 1, 2)$ are the nodal value of $v$ and $v'$ at nodes $j$, respectively. $N_i$ $(i = 1\text{–}4)$ are shape functions and are given by

$$N_1 = \tfrac{1}{4}(1-\xi)^2(2+\xi), \quad N_2 = \frac{S}{8}(1-\xi^2)(1-\xi),$$

$$N_3 = \tfrac{1}{4}(1+\xi)^2(2-\xi), \quad N_4 = \frac{S}{8}(-1+\xi^2)(1+\xi), \tag{20}$$

where $S$ is the current arc length of the centroid axis, and $\xi$ is the nondimensional coordinate defined in eqn (6).

Here, $\bar{v}(\bar{s})$, the initial lateral deflection of the centroid axis, is assumed to have the same form as $v(s)$, and is obtained by adding an overbar for each variable in eqns (19) and (20).

### 2.4. *Element internal nodal force vectors*

The element employed here has three degrees of freedom per node (Fig. 3): these are the translations $u_j$ and $v_j$ $(j = 1, 2)$ in the $x_1$ and $x_2$ directions, respectively, and the counterclockwise rotations $\theta_j$ $(j = 1, 2)$ at nodes $j$. The nodal degrees of freedom for the global coordinate system are the incremental translations $\Delta U_j$ and $\Delta V_j$ $(j = 1, 2)$ in the $X_1$ and $X_2$ directions, respectively, and the incremental counterclockwise rotations $\Delta\theta_j$ $(j = 1, 2)$ at nodes $j$. The nodal forces corresponding to the nodal parameters are the conventional forces and moments as shown in Fig. 3.

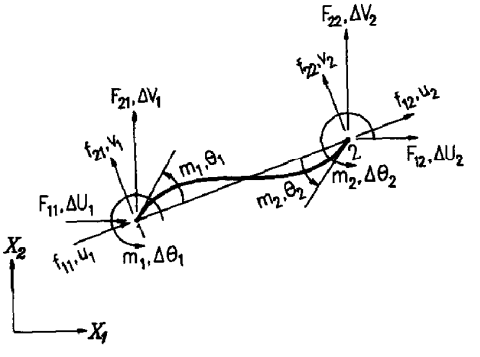


Fig. 3. Nodal parameters and nodal forces.

The element internal nodal forces are obtained from the d'Alembert principle and the virtual work principle. The virtual work principle requires that

$$\delta \mathbf{u}_a^T \mathbf{f}_a + \delta \mathbf{u}_b^{\theta T} \mathbf{f}_b = \int_{\bar{V}} (\delta \epsilon^T \sigma + \rho \delta \mathbf{r}^T \ddot{\mathbf{r}}) \, d\bar{V}, \quad (21)$$

where

$$\delta \mathbf{u}_a = \{\delta u_1, \delta u_2\} \quad (22)$$

$$\delta \mathbf{u}_b^{\theta} = \{\delta v_1, \delta \theta_1, \delta v_2, \delta \theta_2\} \quad (23)$$

$$\mathbf{f}_a = \mathbf{f}_a^d + \mathbf{f}_a^i = \{f_{11}, f_{12}\} \quad (24)$$

$$\mathbf{f}_b = \mathbf{f}_b^d + \mathbf{f}_b^i = \{f_{21}, m_1, f_{22}, m_2\} \quad (25)$$

in which $\mathbf{f}_j^d$ and $\mathbf{f}_j^i$ $(j = a, b)$ are the deformational nodal force vector due to deformations and the inertia nodal force vector, respectively. $\delta\epsilon$ is the variation of $\epsilon$ given in eqn (18). $\sigma = E\epsilon$ is the normal stress, where $E$ is the Young's modulus. $\rho$ is the density, $\delta \mathbf{r}$ is the variation of $\mathbf{r}$ given in eqn (2) with respect to the nodal parameters, and $\ddot{\mathbf{r}} = d^2\mathbf{r}/dt^2$. In this paper, the symbol $(\dot{})$ denotes differentiation with respect to time $t$. $\bar{V}$ is the volume of the undeformed beam. For a curved beam the differential volume $d\bar{V}$ may be expressed as $d\bar{V} = (1 - \bar{\kappa}y)\, dA\, ds/(1 + \epsilon_0)$, where $A$ is the cross section area.

The exact expression of $\mathbf{f}_a$ and $\mathbf{f}_b$ may be obtained by substituting the exact expression of $\delta\epsilon$, $\epsilon$, $\delta \mathbf{r}$, and $\ddot{\mathbf{r}}$ into eqn (21). However, if the element size is properly chosen, the nodal parameters of the element may always be much smaller than unity. Thus only the first order terms of nodal parameters are retained in $\mathbf{f}_a^d$ and $\mathbf{f}_b^d$, and only zeroth order terms of nodal parameters are retained in $\mathbf{f}_a^i$ and $\mathbf{f}_b^i$. However, in order to include the effect of axial force, a second order term of nodal parameters is retained in $\mathbf{f}_b^d$. The approximations $1 + \epsilon_0 \approx 1$, $v' \approx \theta$, and $\cos\theta \approx 1$ are used in the derivation of $\mathbf{f}_a$ and $\mathbf{f}_b$. In order to avoid improper omission in the derivation of $\mathbf{f}_a$ and $\mathbf{f}_b$, these approximations are applied to the exact expression of $\delta\epsilon$, $\epsilon$, $\delta \mathbf{r}$ and $\ddot{\mathbf{r}}$.

From eqns (3)–(9) and (13)–(16), the variation of $\epsilon$ in eqn (18) may be expressed as

$$\delta\epsilon = \frac{1}{1 - \bar{\kappa}y} [(1 - \kappa y)\delta\epsilon_0 - (1 + \epsilon_0) y \delta\kappa], \quad (26)$$

where

$$\delta\kappa = c\delta v'' + c^3 v' v'' \delta v' \quad (27)$$

$$\delta\epsilon_0 = \frac{\delta S}{\bar{S}} = \frac{2\delta l}{\beta \bar{S}} - \frac{2l\delta\beta}{\beta^2 \bar{S}} \quad (28)$$

$$\delta l = \{-1, 1\}^T \{\delta u_1, \delta u_2\} = \mathbf{G}_a^T \delta \mathbf{u}_a \quad (29)$$

$$\delta\beta = -\int_{-1}^{1} cv' \delta v' \, d\xi, \quad (30)$$

in which $\delta v'$ and $\delta v''$ are the variations of $v'$ and $v''$, respectively, with respect to the nodal parameters. From eqns (19) and (20), $\delta v'$ and $\delta v''$ can be obtained as

$$\delta v' = (\delta \mathbf{N}_b'^T)\mathbf{u}_b + \mathbf{N}_b'^T \delta \mathbf{u}_b = -\frac{\delta\epsilon_0}{1 + \epsilon_0} \mathbf{N}_c^T \mathbf{u}_b + \mathbf{N}_b'^T \delta \mathbf{u}_b \quad (31)$$

and

$$\delta v'' = (\delta \mathbf{N}_b''^T)\mathbf{u}_b + \mathbf{N}_b''^T \delta \mathbf{u}_b = -\frac{\delta\epsilon_0}{1 + \epsilon_0} \mathbf{N}_d^T \mathbf{u}_b + \mathbf{N}_b''^T \delta \mathbf{u}_b, \quad (32)$$

where

$$\delta \mathbf{u}_b = \{\delta v_1, \cos\theta_1 \delta\theta_1, \delta v_2, \cos\theta_2 \delta\theta_2\} \quad (33)$$

$$\mathbf{N}_c = \{N_1', 0, N_3', 0\} \quad (34)$$

$$\mathbf{N}_d = \{2N_1'', N_2'', 2N_3'', N_4''\}. \quad (35)$$

Note that due to the definition of the element coordinate system, the values of $v_1$ and $v_2$ are zero. Thus $\mathbf{N}_c^T \mathbf{u}_b = 0$ in eqn (31), and $\mathbf{N}_d^T \mathbf{u}_b = v''$ in eqn (32).

From eqns (27)–(35), using the approximations $1 + \epsilon_0 \approx 1$, $v' \approx \theta$, and $\cos\theta \approx 1$, and retaining all zeroth order terms and one first order term of nodal parameters, $\delta\epsilon$ in eqn (26) may be approximated by

$$\delta\epsilon = \frac{1}{1 - \bar{\kappa}y} \left[ \frac{1}{\bar{S}} \mathbf{G}_a^T \delta \mathbf{u}_a + \mathbf{G}_b^T \delta \mathbf{u}_b - y \mathbf{N}_b''^T \delta \mathbf{u}_b \right], \quad (36)$$

where

$$\mathbf{G}_b = \frac{1}{2} \int_{-1}^{1} v' \mathbf{N}_b' \, d\xi. \quad (37)$$

From eqns (2)–(9), (19), and (20), $\delta \mathbf{r}$ can be expressed as

$$\delta \mathbf{r} = \left\{ \delta u_1 + \frac{\delta S}{2} \int_{-1}^{\xi} \cos\theta \, d\xi - \frac{S}{2} \int_{-1}^{\xi} cv' \delta v' \, d\xi - y\delta v', \delta v - ycv' \delta v' \right\}, \quad (38)$$

where

$$\delta v = (\delta \mathbf{N}_b^T)\mathbf{u}_b + \mathbf{N}_b^T \delta \mathbf{u}_b = \frac{\delta\epsilon_0}{1 + \epsilon_0} \mathbf{N}_e^T \mathbf{u}_b + \mathbf{N}_b^T \delta \mathbf{u}_b \quad (39)$$

and

$$\mathbf{N}_e = \{0, N_2, 0, N_4\}. \quad (40)$$

Substituting eqns (28)–(31), (39), and (40) into eqn (38), using the approximations $1 + \epsilon_0 \approx 1$, $v' \approx \theta$, and

$\cos\theta \approx 1$, and retaining only zeroth order terms of nodal parameters, we may obtain

$$\delta \mathbf{r} = \{\mathbf{N}_a^T \delta \mathbf{u}_a - y\mathbf{N}_b'^T \delta \mathbf{u}_b^\theta, \mathbf{N}_b^T \delta \mathbf{u}_b^\theta\}, \tag{41}$$

where

$$\mathbf{N}_a = \left\{\frac{1-\xi}{2}, \frac{1+\xi}{2}\right\}. \tag{42}$$

From eqns (2)–(9), (19), and (20), the exact expression of $\ddot{\mathbf{r}}$ may be obtained. Using the approximations $1+\epsilon_0 \approx 1$, $v' \approx \theta$, and $\cos\theta \approx 1$, and retaining only zeroth order terms of nodal parameters in the exact expression of $\ddot{\mathbf{r}}$, we may obtain

$$\ddot{\mathbf{r}} = \{a_x, a_y\} = \left\{\mathbf{N}_a^T \ddot{\mathbf{u}}_a + \frac{\bar{S}(1+\xi)}{4}\int_{-1}^{1} (\mathbf{N}_b'^T \ddot{\mathbf{u}}_b)^2 \, d\xi - \frac{\bar{S}}{2}\int_{-1}^{\xi} (\mathbf{N}_b'^T \ddot{\mathbf{u}}_b)^2 \, d\xi + \frac{2y}{\bar{S}}\mathbf{N}_c^T \dot{\mathbf{u}}_b \mathbf{G}_a^T \ddot{\mathbf{u}}_a - y\mathbf{N}_b'^T \ddot{\mathbf{u}}_b, \mathbf{N}_b^T \ddot{\mathbf{u}}_b - y(\mathbf{N}_b'^T \ddot{\mathbf{u}}_b)^2 + \frac{2}{\bar{S}}\mathbf{G}_a^T \ddot{\mathbf{u}}_a \mathbf{N}_c^T \ddot{\mathbf{u}}_b\right\}, \tag{43}$$

where

$$\dot{\mathbf{u}}_a = \{\dot{u}_1, \dot{u}_2\}, \quad \ddot{\mathbf{u}}_a = \{\ddot{u}_1, \ddot{u}_2\} \tag{44}$$

and

$$\dot{\mathbf{u}}_b = \{\dot{v}_1, \dot{\theta}_1, \dot{v}_2, \dot{\theta}_2\}, \quad \ddot{\mathbf{u}}_b = \{\ddot{v}_1, \ddot{\theta}_1, \ddot{v}_2, \ddot{\theta}_2\}. \tag{45}$$

Note that $\dot{\mathbf{u}}_j$ and $\ddot{\mathbf{u}}_j$ ($j = a, b$) are the absolute velocity and acceleration vectors of an element referred to the element coordinates which are obtained from the transformation of the corresponding global velocity and acceleration vectors extracted from the equations of motion of the system using standard procedure [9].

Substituting eqns (18), (36), (38), (41), and (43) into eqn (21), using the approximations $1+\epsilon_0 \approx 1$, $v' \approx \theta$, and $\cos\theta \approx 1$, dropping higher order terms of nodal parameters, and equating the terms in both sides of eqn (21) corresponding to virtual displacement vectors $\delta \mathbf{u}_a$ and $\delta \mathbf{u}_b^\theta$, respectively, we may obtain

$$\mathbf{f}_a^d = \frac{E}{\bar{S}}\int \epsilon \, dA \, ds \mathbf{G}_a \tag{46}$$

$$\mathbf{f}_b^d = \frac{E}{2}\int \epsilon \, dA \, ds \int_{-1}^{1} \mathbf{N}_b' \mathbf{N}_b'^T \, d\xi \mathbf{u}_b - E\int y\epsilon \mathbf{N}_b'' dA \, ds \tag{47}$$

$$\mathbf{f}_a^i = \int \rho(1-\bar{\kappa}y) a_x \mathbf{N}_a \, dA \, ds \tag{48}$$

$$\mathbf{f}_b^i = \int \rho(1-\bar{\kappa}y)(-ya_x \mathbf{N}_b' + a_y \mathbf{N}_b) \, dA \, ds. \tag{49}$$

### 2.5. *Element matrices*

The element stiffness matrices and mass matrices may be obtained by differentiating the element nodal force vectors in eqns (46)–(49) with respect to nodal parameters, and time derivatives of nodal parameters. However, element matrices are only used to obtain predictors and correctors for incremental solutions of nonlinear equations in this study. Approximate element matrices can meet these requirements. Thus, the element matrices used in [9] for a straight beam are adopted here for simplicity.

### 2.6. *Equations of motion*

The nonlinear equations of motion may be expressed by

$$\boldsymbol{\varphi} = \mathbf{F}^I + \mathbf{F}^D - \mathbf{P} = \mathbf{0}, \tag{50}$$

where $\boldsymbol{\varphi}$ is the unbalanced force among the inertia nodal force $\mathbf{F}^I$, deformational nodal force $\mathbf{F}^D$, and the external nodal force $\mathbf{P}$. $\mathbf{F}^I$ and $\mathbf{F}^D$ are assembled from the element nodal force vectors in eqns (46)–(49), which must be transformed from element coordinate system to global coordinate system before assemblage using standard procedure.

In this paper, a weighted Euclidean norm of the unbalanced force is employed for the equilibrium iterations, and is given by

$$e = \frac{\|\boldsymbol{\varphi}\|}{N} \leqslant e_{tol}, \tag{51}$$

where $N$ is number of the equations of the system; $e_{tol}$ is a prescribed value of error tolerance. The error tolerance is set to $10^{-6}$ in this paper.

## 3. APPLICATIONS

An incremental iterative method based on the Newmark direct integration method [9, 18] and the Newton–Raphson method is employed. The procedure used here to determine the deformational nodal rotations for individual elements is the same as that proposed in [19] and is not repeated here.

In order to investigate the effect of the initial curvature on the dynamic response, three examples are studied using the curved Euler beam (CEB) element proposed here and the straight Euler beam (SEB) element proposed by Hsiao *et al.* [14].

### 3.1. *Clamped semicircular arch* (R/h = 67.115)

A clamped semicircular arch (Fig. 4) subjected to a central concentrated step loading $P$ of magnitude 700 lb is analyzed. The geometry and material properties of the arch are: $h = 1$ in., width = 1 in., $E = 10^7$ psi, and $\rho = 2.44 \times 10^{-4}$ lb $-$ sec$^2$/in$^4$. Because of symmetry, only half of the arch is analyzed using 15 elements. The time step size is chosen to be $2.5 \times 10^{-4}$ sec. The time histories of the vertical displacement and the strain of the top edge at the loading point are shown in Figs 5 and 6, respectively.

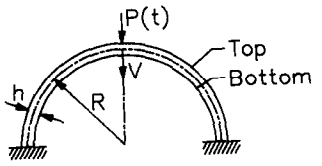


Fig. 4. Semicircular circular arch.

As expected, the results of SEB elements (not shown) are nearly identical with the results of CEB elements for this slender curved beam structure. Also shown in Fig. 5 are the results of [3]. Very good agreement between these two solutions is observed.

### 3.2. *Clamped semicircular arch* (R/h = 5)

The clamped semicircular arch considered here is moderately thick. This arch is subjected to a central concentrated loading $P(t)$ as follows.

$$P(t) = \begin{cases} 2000[1 - \cos(\pi t/0.0003)]\ \text{lb} & 0 \leqslant t \leqslant 0.0003\ \text{sec} \\ 4000\ \text{lb} & t > 0.0003\ \text{sec}. \end{cases}$$

The geometry and material properties of the arch are the same as those given in the first example. Because of symmetry, only half of the arch is analyzed using 15 elements. The time step size is chosen to be $2 \times 10^{-6}$ sec. The time histories of the vertical displacement and the strains at the loading point are shown in Figs 7 and 8. $\epsilon_t$, $\epsilon_c$, and $\epsilon_b$ in Fig. 8 denote the strains on the top edge, centroid, and bottom edge, respectively. As can be seen, the discrepancy between the strains obtained by using the CEB and SEB elements is not negligible.

### 3.3. *Quarter-circular arch*

This example considered is a quarter-circular arch rotating horizontally about a vertical axis passing through one end as shown in Fig. 9. The geometry of the arch is: $R/h = 5$, $h = 5$ in., and width = 5 in. The material properties of the arch are the same as those given in the first example. This arch is subjected to a prescribed rotation angle $\psi(t)$ at one end as follows.

$$\psi(t) = \begin{cases} \dfrac{25}{0.016}\left[\dfrac{t^2}{2} + \left(\dfrac{0.016}{2\pi}\right)^2\left(\cos\dfrac{2\pi t}{0.016} - 1\right)\right]\text{rad} & 0 \leqslant t \leqslant 0.016\ \text{sec} \\ (25t - 0.2)\text{rad} & t > 0.016\ \text{sec}. \end{cases}$$

The beam is discretized using 15 elements. The time step size is set to $10^{-4}$ sec. The time histories of the tip displacements $U$ and $V$, which are defined in Fig. 9, are shown in Fig. 10. The time histories of the strains at root are shown in Fig. 11. $\epsilon_t$, $\epsilon_c$, and $\epsilon_b$ in Fig. 11 denote the strains on the top edge, centroid, and bottom edge respectively. It is observed that the tip displacments obtained by using the CEB and SEB elements are nearly identical. However, the discrepancy between the strains obtained by using the CEB and SEB elements is not negligible.

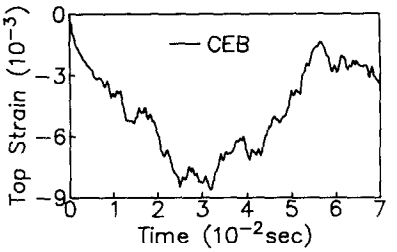


Fig. 6. Time history for tip strain.

## 4. CONCLUSIONS

This paper has described a consistent finite element formulation for the dynamic analysis of a planar curved Euler beam. The Euler–Bernoulli hypothesis and the initial curvature are properly considered for the kinematics of curved beams. Both the inertia nodal forces and deformational nodal forces are systematically derived by consistent linearization of the fully geometrically nonlinear beam theory using the d'Alembert principle and the virtual work principle. In conjunction with the co-rotational formulation, the higher order terms of nodal parameters in element nodal forces are consistently neglected. From the numerical examples studied, it is found that the effects of the initial curvature on the dynamic response of strains are not negligible for moderately thick curved beam structures.

It is believed that the consistent co-rotational formulation for a curved beam element presented

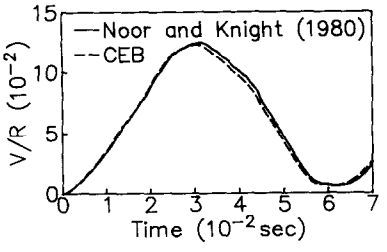


Fig. 5. Time history for tip displacement.

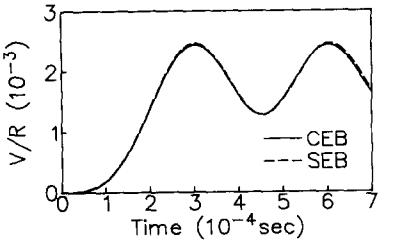


Fig. 7. Time history for tip displacement.

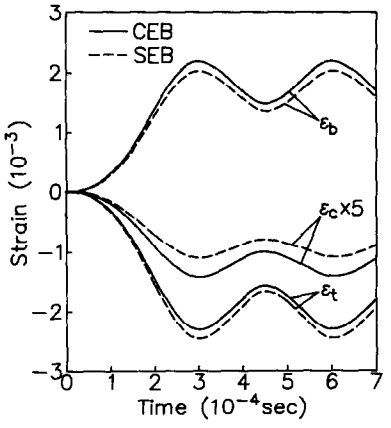


Fig. 8. Time history for tip strains.

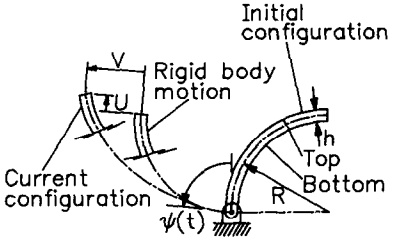


Fig. 9. Quarter-circular arch.

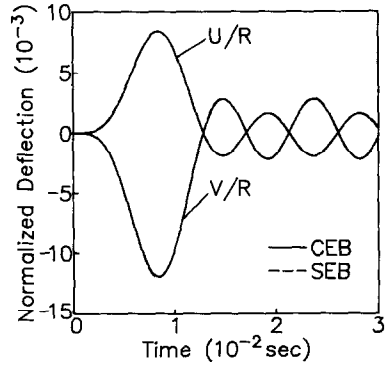


Fig. 10. Time history for displacement components $U$ and $V$.

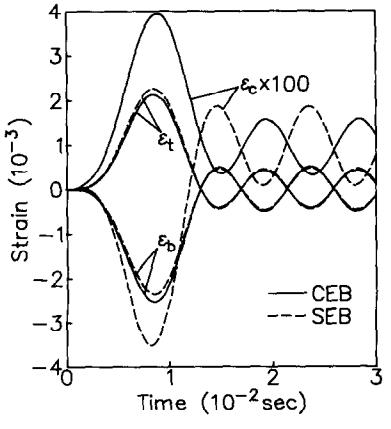


Fig. 11. Time history for root strains.

here may represent a valuable engineering tool for the dynamic analysis of planar curved beam structures.

*Acknowledgment*—The research was sponsored by the National Science Council, Republic of China, under the contract NSC79-0401-E009-15.

## REFERENCES

1. D. P. Mondkar and G. H. Powell, Finite element analysis of no-linear static and dynamic response. *Int. J. Numer. Meth. Engng* **11,** 499–520 (1977).
2. J. O. Song and E. J. Haug, Dynamic analysis of planar flexible mechanisms. *Comput. Meth. Appl. Mech. Engng* **24,** 359–381 (1980).
3. A. K. Noor and N. F. Knight, Nonlinear dynamic analysis of curved beams. *Comput. Meth. Appl. Mech. Engng* **23,** 225–251 (1980).
4. M. Badlani and A. Midha, Member initial curvature effects on the elastic slider-crank mechanism response. *ASME J. Mech. Des.* **104,** 159–167 (1982).
5. T. Y. Yang and S. Saigal, A simple element for static and dynamic response of beams with material and geometric nonlinearities. *Int. J. Numer. Meth. Engng* **20,** 851–867 (1984).
6. C. J. Simo and L. Vu-Quoc, The role of non-linear theories in transient dynamic analysis of flexible structures. *J. Sound Vibr.* **119,** 487–508 (1987).
7. T. R. Kane, R. R. Ryan and A. K. Banerjee, Dynamics of a cantilever beam attached to a moving base. *J. Guid. Control Dyn.* **10,** 139–151 (1987).
8. S. K. Ider and F. M. L. Amirouche, Nonlinear modeling of flexible multibody systems dynamics subjected to variable constraints. *ASME J. appl. Mech.* **56,** 444–450 (1989).
9. K. M. Hsiao and J. Y. Jang, Nonlinear dynamic analysis of elastic frames. *Comput. Struct.* **33,** 1057–1063 (1989).
10. D. F. Bartolone and A. A. Shabana, Effect of beam initial curvature on the dynamics of deformable multibody system. *Mech. Machine Theory* **24,** 421–429 (1989).
11. Z. Yang and J. P. Sadler, Large-displacement finite element analysis of flexible linkages. *ASME J. Mech. Des.* **112,** 175–182 (1990).
12. K. M. Hsiao and J. Y. Jang, Dynamic analysis of planar flexible mechanisms by co-rotational formulation. *Comput. Meth. appl. Mech. Engng* **87,** 1–14 (1991).
13. K. M. Hsiao and R. T. Yang, Dynamic behaviour of planar flexible mechanisms with member initial curvature. In *Structural Dynamics: Recent Advances* (Edited by M. Petyt, H. F. Wolfe and C. Mei). Elsevier Applied Science, London (1991).
14. K. M. Hsiao, R. T. Yang and A. C. Lee, A consistent finite element formulation for nonlinear dynamic analysis of planar beam. *Int. J. Numer. Meth. Engng* **37,** 75–89 (1994).
15. A. P. Boresi and O. M. Sidebottom, *Advanced Mechanics of Materials.* John Wiley, New York (1985).
16. D. H. Hodges, Proper definition of curvature in nonlinear beam kinematics. *AIAA Jl* **22,** 1825–1827 (1984).
17. T. J. Chung, *Continuum Mechanics.* Prentice-Hall, Englewood Cliffs, NJ (1988).
18. K. J. Bathe, *Finite Element Procedures in Engineering Analysis.* Prentice-Hall, Englewood Cliffs, NJ (1982).
19. K. M. Hsiao and F. Y. Hou, Nonlinear finite element analysis of elastic frames. *Comput. Struct.* **26,** 693–701 (1987).